Local Structural Distortions below and above the Antiferrodistortive Phase Transition

B. Rechav,[1] Y. Yacoby,[1] E. A. Stern,[2] J. J. Rehr,[2] and M. Newville[2]
[1]*Racah Institute of Physics, Hebrew University of Jerusalem, Jerusalem, Israel 91904*
[2]*Physics Department FM-15, University of Washington, Seattle, Washington 98195*
(Received 1 September 1993)

Quantitative measurements of oxygen octahedra local rotation angles are reported for the antiferrodistortive type perovskites, $Na_{0.82}K_{0.18}TaO_3$ and $NaTaO_3$. The results were obtained using a detailed analysis of x-ray absorption fine structure spectra. These results show that the oxygen octahedra rotation angle at the peak of the rotation angle distribution function of an antiferrodistortive crystal is nonzero and large, hundreds of degrees above the transition temperature.

PACS numbers: 61.10.Lx, 64.70.Kb

Antiferrodistortive phase transitions (APT), involving the rotation of oxygen octahedra in oxygen perovskite crystals, have long been considered exemplary displacive transitions [1]. In a crystal undergoing a pure displacive transition, the distortion at the peak of the local distortion distribution function is expected to go to zero above T_c. In this Letter we present x-ray absorption fine structure (XAFS) results, which determine quantitatively the local rotation angles of the oxygen octahedra of an antiferrodistortive crystal. The results show that the angle at the peak of the local rotation angle distribution function is nonzero and large, hundreds of degrees above T_c. In $Na_{0.82}K_{0.18}TaO_3$ ($T_c = 490$ K), the local rotation angle at 823 K is smaller by only 25% than the angle measured at room temperature. The decrease is gradual, showing no extra dependence near the transition.

APT's have been intensively investigated and the results are summarized in a number of excellent reviews [2,3]. So far, the main emphasis has been on the critical behavior of these systems near T_c. The critical behavior is manifested in the critical exponent of the order parameter [2], in a soft mode frequency that tends to saturate close to the transition temperature [4] and in a critical increase of a central peak observed in both neutron [4] and x-ray diffraction [5]. The existence of the central peak suggests that local distortions from the high symmetry structure are present also above T_c. However, there is no quantitative information on their size and it is not clear if the distortions are intrinsic or extrinsic [3,5].

Local structural distortions above T_c have attracted much interest in another class of structural phase transitions, namely, in ferroelectric transitions. Various experiments including diffuse scattering [6], optical [7,8], resonance [9], and XAFS [10,11] measurements established that contrary to previous convictions the local structure is distorted not only below but also above the ferroelectric phase transition. These results indicate that ferroelectric transitions have an essential element of order-disorder.

XAFS has unique advantages for the determination of local structure in crystals [12]: It has the highest resolution in the measurement of the pair distribution function in disordered materials; it is insensitive to long range orientational disorder and in certain cases it can provide bond angles in addition to bond lengths. The characteristic absorption time of an x-ray photon is $\sim 10^{-16}$ sec. Thus, XAFS reveals the atomic position distribution function rather than the time averaged structure. This is the only technique, so far, that has provided quantitative information on the disordered distortions above T_c in ferroelectric crystals [10,11].

Two crystals were investigated—$Na_{0.82}K_{0.18}TaO_3$ (KNTO) and $NaTaO_3$ (NTO). In this Letter we shall concentrate on KNTO which has a lower T_c and mention the NTO for comparison only. NTO has four phases —cubic, tetragonal, and two orthorhombic phases [13]. The transition temperatures are 900, 820, and 750 K, respectively. Below 900 K the oxygen octahedra rotate around axes equivalent to [001], [011], and [111], respectively [14]. At room temperature the rotation angles were found to be 10.4° by x-ray [15] and 12.5° by neutron diffraction [14].

In mixed $Na_xK_{1-x}TaO_3$, the APT temperature decreases fast with decreasing Na concentration, and at $x = 0.82$ the transition temperature found from birefringence measurements is ~ 490 K. At room temperature the crystal is orthorhombic [16].

A single KNTO crystal was obtained from the late Dr. A. Linz from MIT and the NTO powder was purchased from ICN. Hand ground powders of both materials were sifted through 400 mesh grid and examined under a microscope. Crystallite sizes were mostly in the range 1–10 μm, so thickness effects and small size effects were avoided. The powders were mixed with graphite powder in order to obtain manageable quantities and pressed to form rigid pellets, about 1 mm thick.

The measurements were done at beam line X11-A at NSLS. We used the Ta L_{III} edge, with a midstep energy of 9881 eV. Above the edge the samples had an absorption coefficient of $\mu x \simeq 2$, and an edge step of 0.4. Pure NTO was measured at 300, 373, 473, 573, 673, 723, 773, and 823 K, and KNTO was measured at 300, 373, 433, 473, 523, 573, 723, and 823 K, all stabilized with an accuracy of 2 K. Standard experimental procedures were followed to minimize distortions and other systematic er-

0031-9007/94/72(9)/1352(4)$06.00

rors. The overall quality of the measurements is good, as can be seen in Fig. 1.

The analysis of the data is based on fitting the Fourier transforms of theoretical calculations to those of experimental spectra in a specified range in r space, where r represents the distance to the probe [10,17]. Only details relevant to the present analysis are provided here.

The background of the experimental spectrum was removed using the method described by Newville *et al.* [18]. It was approximated by a cubic spline function, determined by eight points evenly spread in the photoelectron energy space. The Fourier transform of the background was found to be negligible with respect to the XAFS signal above 1.0 Å, so this was chosen as the lower bound of the fitting range, $r_{\min}$.

XAFS spectra can be schematically expressed as a sum of contributions in the following way [17]:

$$\chi(k) = \mathrm{Im}\sum_{\eta} n_\eta F_\eta(k)\exp[i(kL_\eta + \Theta_\eta(k) + C_\eta/k)] \times \exp(-2k^2\sigma_\eta^2)\exp(-L_\eta/\lambda_\eta). \quad (1)$$

Here, η is the photoelectron scattering path index; n is the number of equivalent paths; k and L are the wave number and total scattering path length of the x-ray excited photoelectron, respectively, and σ^2 is the effective mean squared relative displacement. $F(k)$ and $\Theta(k)$ are the scattering amplitude and phase functions. These functions were calculated using the *ab initio* FEFF5 code of Rehr, Zabinsky, and Albers [19]. Finally, C/k and $(-L/\lambda)$ are phase shift and mean free path correction terms.

Oxygen octahedral rotations around [111] type axes affect the XAFS spectrum in two major ways: (1) The rotation of the center oxygen octahedron moves the nearest neighbor oxygens away from the line connecting the probe and third neighbor Ta atoms. This changes significantly the collinear double and triple scattering from the third Ta shell [20]. For small rotation angles the changes in these contributions are quadratic with angle and are therefore proportional to the second moment of the rotation angle distribution function α_f^2. (2) The rotation of the adjacent octahedra by an angle ϕ_4 splits the fourth neighbor oxygen shell O_4 into two subshells with unequal distances to the probe. This affects the XAFS spectrum directly through the exponential term in Eq. (1).

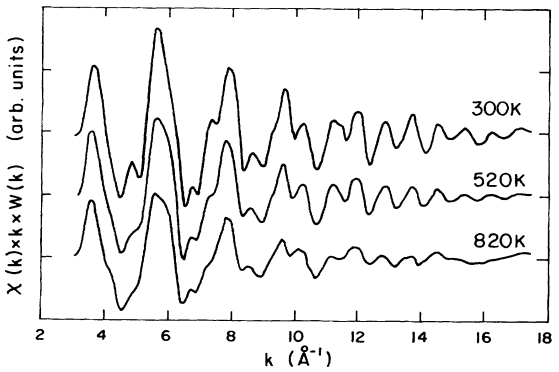

FIG. 1. The normalized x-ray absorption coefficient of KNTO, multiplied by the photoelectron wave number k and by the window function $W(k)$, as a function of k, for three different temperatures.

In order to analyze both effects, the upper bound of the fitting range $r_{\max}$, was set to 4.2 Å, for a total path length of 8.4 Å. This range includes the fourth shell. All scattering paths with a total length shorter than 12 Å were calculated, and those with significant contribution within the fitting range were included in the fit. The final set consisted of single, double, and triple scattering paths, the longest being 2.7 times the unit cell dimension, namely, 10.8 Å.

The XAFS spectra were expressed in terms of seven temperature dependent and eight temperature independent parameters:

(a) Temperature dependent parameters: (i) The parameters α_f^2 and ϕ_4 defined above. Using two different parameters to describe two coupled rotations introduces an internal consistency check of the analysis. (ii) Five mean squared relative displacement (σ^2) parameters for the four single scattering configurations (separate σ^2 for Ta-Na and Ta-K bonds). The σ^2 of the multiple scattering paths were expressed in an approximate way in terms of the single scattering configuration σ^2.

(b) Temperature independent parameters: (i) A linear lattice thermal expansion coefficient (TEC). (ii) The energy threshold parameter E_0, which fixes the $k=0$ point on the energy scale. (iii) Four phase shift corrections of the form C_η/k for the atoms in the three outer shells. The phase corrections of the multiple scattering configurations use these same parameters [10]. (iv) Two mean-free-path corrections of the form $\exp(-L/\lambda)$, one for paths involving atoms in the first shell and one for all other paths.

The values of the temperature independent parameters, with the exception of TEC, were adjusted so as to optimize the fits at all temperatures and for both materials.

The total number of the experimentally independent relevant points $N = 2\Delta r \Delta k/\pi$, where Δk is the k range of valid data and $\Delta r = r_{\max} - r_{\min}$. In our experiments $N \sim 28$ and is large compared to the seven temperature dependent parameters and is even large compared to the total number of fifteen parameters.

Prior to the fit, both experimental and calculated spectra were multiplied by k to emphasize the high k region, and further multiplied by a half sine envelope $W(k)$ to suppress ringing in the Fourier transform [10]. The experimental and theoretical spectra were Fourier transformed and fitted in r space. Several examples of the KNTO spectra at temperatures both below and above T_c are shown in Fig. 2. These fits are typical of all spectra in both materials and as can be seen are very good.

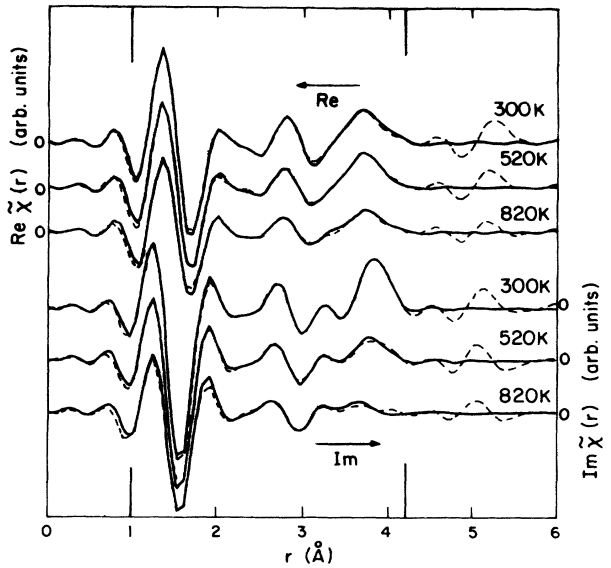

FIG. 2. The real part, top, and imaginary part, bottom, of the Fourier transform of the XAFS spectrum of KNTO, as a function of the distance to the probe r, for three different temperatures. The vertical lines represent the fitting range.

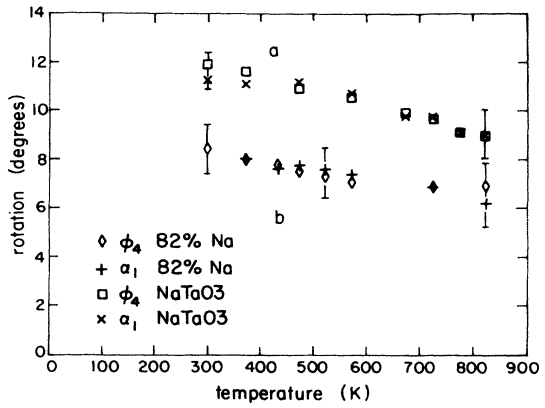

FIG. 3. The rotation angle of the octahedron associated with the O_4 oxygens, ϕ_4, and the square root of the second moment of the rotation distribution function of the center octahedron, α_1, as a function of temperature for $Na_{0.82}K_{0.18}TaO_3$ and $NaTaO_3$.

The phase correction coefficients used were 1.5, 5.0, 5.0, and -1.5 rad/Å^{-1} for Na, K, Ta, and O_4, respectively. Similar correction parameters were found in the analysis of XAFS spectra of various standard materials. Both mean-free-path corrections were found to be quite small with $\lambda = 33$ Å. E_0 was found to be 13 eV above the nominal absorption edge at 9881 eV. The cell dimensions in NTO were equal to the x-ray results to within 0.01 Å and the thermal expansion coefficients were $3(3)\times10^{-5}$ and $1.4(0.7)\times10^{-5}$ Å/deg for NTO and KNTO, respectively. The temperature dependence of the σ^2 was found to be monotonic, without any anomalous behavior near T_c. They fit well the Einstein model, with static disorder parameter $\sigma_0^2 = 3(1)\times10^{-3}$ Å^2 for the fourth shell, and with Einstein temperatures 594(15), 275(30), 240(10), and 500(130) K for the Ta-O_1, Ta-Na, Ta-Ta, and Ta-O_4 bonds, respectively. These results will be discussed in greater detail elsewhere.

The rotation angle of the adjacent octahedra associated with O_4 oxygens ϕ_4 and the root of the second moment of the rotation angle distribution function of the center oxygen octahedron α_1 are obtained directly from the analysis and are shown in Fig. 3. The rotation angle of the center oxygen octahedron ϕ_1 is related to α_1 through $\phi_1 \simeq \alpha_1 - \sigma_\phi^2/2\alpha_1$, where σ_ϕ^2 are the mean squared librations around the ϕ_1 positions. Estimating σ_ϕ^2 from σ^2 of the fourth neighbor oxygens shows that ϕ_1 is about 1° smaller than α_1. Thus the two rotation angles ϕ_1 and ϕ_4 agree within the error brackets seen in Fig. 3.

The error brackets of the parameters were carefully estimated using a method which takes into account random noise effects and experimental and theoretical systematic errors. We find that systematic errors are dominant. Consequently the error brackets are much larger than the scatter in parameter values.

The low temperature rotation angle that we measure in NTO, $\phi_1 = 11.5(1.0)°$, is in good agreement with the x-ray [15] 10.4° and the neutron [14] 12.5° results. According to neutron diffraction [14], the average rotation at 803 K is 7° about the [011] axis. We found that our data at 823 K can also be fitted to a model with [011] type rotations and the fit quality is about as good. But the local rotation angle that we measure, 9.5(1.0)°, is about 2.5° larger than the value found in neutron diffraction. In the following we discuss only rotations about [111] type axes.

σ_ϕ, extracted from σ^2 of the fourth shell oxygens, increases monotonically and is 4° at 823 K. The results in Fig. 3 show that the octahedra rotation angles decrease gradually with temperature, with no anomalous behavior in the vicinity of the transition. Yet even 330 K above T_c of KNTO, $\phi_4 = 6.9°$ and is larger than σ_ϕ. Thus the fourth shell is clearly split at this temperature, and the distribution function of the rotation angle has a clear peak far above zero.

To further test this conclusion, we tried to fit the 823 K KNTO data to a simple cubic structure by forcing $\phi_4 = 0$. The fit quality was 2 times worse and α_1 as well as the Ta-O_4 σ^2 were very large, 6.9 and 0.07 Å^2, respectively. The large mean squared displacements attempt to compensate for the zero rotations imposed in this model.

The results in Fig. 3 show that within the experimental errors, the difference between the rotation angles of the two crystals is essentially constant. Even at the highest temperature the rotation angles are more than 75% of their values at room temperature. This suggests that the rotation angles in pure NTO also persist at temperatures

above the transition to the cubic phase. Furthermore, if the transitions are of second order, the average rotation angles would follow a Landau or renormalized type of behavior. The data clearly do not follow this sort of behavior, suggesting that the local and average structures differ even below the transition temperature. The growing difference between the two on the approach to T_c is expected to manifest itself in unusually large anisotropic thermal factors in the diffraction pattern, as was indeed reported [14].

The results presented in this paper lead to several conclusions and implications:

(1) The local rotations we observe above T_c are not defect or surface strain induced, because the rotation angle distribution function is quite slowly peaked around one value, while defects would tend to smear it. It has been shown that close to T_c, x-ray diffraction is strongly affected by defects or by proximity to strained surfaces [5]. In contrast to x-ray diffraction, the local rotations we measure are weakly temperature dependent. We suggest that defects and surface strains may induce some order close to T_c, leading to an increase in x-ray diffraction intensity, but they do not induce the local rotations.

(2) We have shown that the local and average rotations are different in a large temperature range both above and below T_c. Thus, the rotations are necessarily disordered above T_c, and partially disordered below it. Since each octahedron shares its oxygens with others, and the octahedra are fairly rigid, the rotation of one of them about a [111] type axis results in the rotations of neighboring octahedra in a cog-wheel-like coupling. However, since the sense and axes of rotation are partially arbitrary, we suggest that the disorder would manifest itself primarily through this arbitrariness.

(3) We suggest that the microscopic mechanism producing the rotations should be reinvestigated. It is clear that the condensation of the soft mode is related to the formation of long range ordered rotations, but it does not create the local rotations. Models describing the existence of intrinsic distortions in the cubic phase of crystals undergoing APT's can be relevant to the disordered distortions observed in our experiments.

[1] E. Pytte and J. Feder, Phys. Rev. **187**, 1077 (1969); J. Feder and E. Pytte, Phys. Rev. B **1**, 4803 (1970).
[2] K. A. Müller, in *Local Properties at Phase Transitions*, edited by K. A. Müller and A. Rigamonti (North-Holland, Amsterdam, 1976), Chap. 2, and references therein.
[3] R. A. Cowley, Adv. Phys. **29**, 1 (1980); A. D. Bruce, Adv. Phys. **29**, 111 (1980); A. D. Bruce and R. A. Cowley, Adv. Phys. **29**, 219 (1980).
[4] S. M. Shapiro, J. D. Axe, G. Shirane, and T. Riste, Phys. Rev. B **6**, 4332 (1972).
[5] S. R. Andrews, J. Phys. C **19**, 3721 (1986).
[6] R. Comes, R. Curra, F. Denoyer, M. Lambert, and A. M. Quittet, Ferroelectrics **12**, 3 (1976).
[7] A. M. Quittet, M. Lambert, and A. Guinier, Solid State Commun. **12**, 1053 (1973).
[8] Y. Yacoby, Z. Phys. B **31**, 275 (1978).
[9] F. Borsa, U. T. Höchli, J. J. Van der Klink, and D. Rytz, Phys. Rev. Lett. **45**, 1884 (1980).
[10] O. Hanske-petitpierre, Y. Yacoby, J. Mustre-deleon, E. A. Stern, and J. J. Rehr, Phys. Rev. B **44**, 6700 (1991).
[11] Q. T. Islam and B. A. Bunker, Phys. Rev. Lett. **59**, 2701 (1987).
[12] E. A. Stern and S. M. Heald, in *Handbook on Synchrotron Radiation*, edited by E. E. Coch (North-Holland, New York, 1983), Vol. 1.
[13] I. G. Ismailzade, Kristallografiya **7**, 718 (1963) [Sov. Phys. Crystallogr. **7**, 584 (1963)].
[14] M. Ahtee and C. N. W. Darlington, Acta Crystallogr. B **36**, 1007 (1980).
[15] M. Ahtee and L. Unonius, Acta Crystallogr. A **33**, 150 (1977).
[16] T. G. Davis, Phys. Rev. B **5**, 2530 (1972).
[17] J. Muster, Y. Yacoby, E. A. Stern, and J. J. Rehr, Phys. Rev. B **42**, 10843 (1990).
[18] M. Newville, P. Livins, Y. Yacoby, J. J. Rehr, and E. A. Stern, Phys. Rev. B **47**, 14126 (1993).
[19] J. J. Mustre, S. I. Zabinsky, and R. C. Albers, J. Am. Chem. Soc. **113**, 5135 (1991); J. J. Rehr, S. I. Zabinsky, and R. C. Albers, Phys. Rev. B **41**, 8139 (1990).
[20] B.-K. Teo, J. Am. Chem. Soc. **103**, 3990 (1981).